Diffraction of Plane Waves by a Strip in an Unbounded Gyrotropic or Biisotropic Space: Oblique Incidence

J. L. Tsalamengas, *Member, IEEE*

Abstract—**Diffraction of plane waves obliquely incident on a perfectly conducting strip of infinite length, which is embedded in an unbounded gyrotropic or bi-isotropic space, is studied. To this end, a system of two singular integral-integrodifferential equations of the first kind is derived following two different methods. This system is efficiently discretized independently using two recently developed direct singular integral equation techniques. Analytical expressions are presented for the far- and near-scattered fields, along with typical numerical results.**

Index Terms—**Electromagnetic scattering.**

I. INTRODUCTION

ANISOTROPIC media are widely used in a variety of applications such as ionospheric research, crystal physics, integrated optics, geophysical exploration, reciprocal and nonreciprocal microwave and millimeter wave devices, etc. Biisotropic media are also potentially useful in a broad field of applications. Examples are radar cross-section reduction and control, design of high-efficiency microstrip antennas and arrays, design of radomes, guiding devices and couplers, and development of microwave and photonic lenses (refer to [1], [2] for extensive lists of pertinent works).

Connected with unbounded anisotropic or biisotropic spaces, this paper studies diffraction of plane waves obliquely incident on embedded vanishingly thin perfectly conducting strips of infinite length. The strong similarities, physical as well as mathematical, that exist between these two problems enable their treatment along parallel lines as outlined in Sections II and III.

For the analysis a system of two singular integral-integrodifferential equations (SIE-SIDE) of the first kind is derived using independently two different approaches (a spectral-domain technique and a space-domain Green's function method). This system, having the induced surface current densities as the unknowns, is efficiently discretized following two different moment-method oriented direct SIE techniques recently developed in [3]. Analytical expressions are derived both for the far- and near-scattered fields and numerical results are presented for several cases.

Manuscript received August 1, 1994; revised March 27, 1998.

The author is with the Department of Electrical and Computer Engineering, National Technical University of Athens, Athens, GR-157 73 Greece.

Publisher Item Identifier S 0018-926X(98)05785-8.

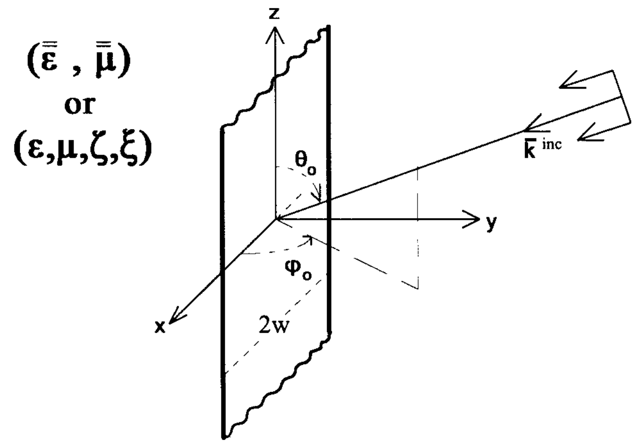

Fig. 1. Geometry of the problem.

II. SCATTERING BY A STRIP IN AN ANISOTROPIC SPACE

Fig. 1 shows a vanishingly thin perfectly conducting strip at $y = 0$, $|x| \leq w, -\infty < z < +\infty$ in an unbounded lossless homogeneous gyrotropic space $(\bar{\bar{\epsilon}}, \bar{\bar{\mu}})$. The strip- and anisotropy-axes are taken to coincide, i.e.,

$$\begin{aligned}\bar{\bar{\epsilon}} &= \epsilon_0[\epsilon_1(\hat{x}\hat{x} + \hat{y}\hat{y}) - j\epsilon_2(\hat{x}\hat{y} - \hat{y}\hat{x}) + \epsilon_3\hat{z}\hat{z}]\\ \bar{\bar{\mu}} &= \mu_0[\mu_1(\hat{x}\hat{x} + \hat{y}\hat{y}) - j\mu_2(\hat{x}\hat{y} - \hat{y}\hat{x}) + \mu_3\hat{z}\hat{z}]\end{aligned} \tag{1}$$

$[\epsilon_i \in R, \mu_i \in R$ $(i = 1, 2, 3)$-lossless condition; ϵ_0, μ_0 refer to free-space].

Assume an obliquely incident plane wave impinging on the strip. The induced surface current density $\overline{J} = \hat{x}J_x + \hat{z}J_z$ gives rise to the scattered field. The z dependence of all these field quantities is $e^{-j\beta z}$ where β is specified by the incident wave as outlined in Section II-B below.

In the limiting case of a perfectly conducting half-plane and for several orientations of the anisotropy axis, this diffraction problem has been treated in [4] and [5] using the Wiener–Hopf–Hilbert method. The present finite strip problem will be formulated in terms of a system of two SIE-SIDE as follows.

A. Basic Equations

Solutions of the source-free Maxwell's equations $\nabla \times \overline{E} = -j\omega\bar{\bar{\mu}}\overline{H}$, $\nabla \times \overline{H} = j\omega\bar{\bar{\epsilon}}\overline{E}$ that vary as $e^{j(\omega t - \beta z)}$ (such as the incident and scattered waves, for instance) can be expressed in terms of their longitudinal components E_z and H_z. The latter satisfy coupled second-order differential equations

$$\begin{aligned}(\nabla_t^2 + k_\epsilon^2)E_z &= -j\omega\mu_0\mu_3\nu H_z\\ (\nabla_t^2 + k_\mu^2)H_z &= j\omega\epsilon_0\epsilon_3\nu E_z\end{aligned} \tag{2}$$

$$\begin{aligned}k_\epsilon^2 &= -\beta^2\frac{\epsilon_3}{\epsilon_1} + k_0^2\epsilon_3\mu_e, \quad k_\mu^2 = -\beta^2\frac{\mu_3}{\mu_1} + k_0^2\mu_3\epsilon_e\\ p_e &= \frac{p_1^2 - p_2^2}{p_1}\ (p \equiv \epsilon, \mu), \quad \nu = \beta\left(\frac{\epsilon_2}{\epsilon_1} + \frac{\mu_2}{\mu_1}\right)\end{aligned} \tag{3}$$

where $\nabla_t = \hat{x}(\vartheta/\vartheta x) + \hat{y}(\partial/\partial y)$, $k_0^2 = \omega^2\epsilon_0\mu_0$. In terms of E_z and H_z, which play the role of scalar potentials, the transverse components are given by

$$\begin{aligned}\begin{pmatrix}\overline{E}_t\\ \overline{H}_t\end{pmatrix} &= \begin{pmatrix}\nu & \upsilon\\ -\hat{\upsilon} & \nu\end{pmatrix}^{-1}\\ &\cdot \begin{pmatrix}\hat{z}\times\nabla_t + j(\mu_2/\mu_1)\nabla_t & \dfrac{\beta}{\omega\epsilon_0\epsilon_1}\nabla_t\\ -\dfrac{\beta}{\omega\mu_0\mu_1}\nabla_t & \hat{z}\times\nabla_t + j(\epsilon_2/\epsilon_1)\nabla_t\end{pmatrix}\\ &\cdot \begin{pmatrix}E_z\\ H_z\end{pmatrix}\end{aligned} \tag{4}$$

$$\upsilon = jk_\epsilon^2/(\omega\epsilon_0\epsilon_3), \quad \hat{\upsilon} = jk_\mu^2/(\omega\mu_0\mu_3). \tag{5}$$

B. Incident Field

Let $(\overline{E}^{\text{inc}}, \overline{H}^{\text{inc}}) = (\overline{E}_0, \overline{H}_0)\exp(j\overline{k}^{\text{inc}}\cdot\overline{r})$ be the incident plane wave propagating in the direction of

$$\begin{aligned}\overline{k}^{\text{inc}}(k, \vartheta_0, \phi_0) &= k_x\hat{x} + k_y\hat{y} - \beta\hat{z}; \quad k_x = k\sin\vartheta_0\cos\phi_0,\\ k_y &= k\sin\vartheta_0\sin\phi_0, \quad \beta = -k\cos\vartheta_0\end{aligned} \tag{6}$$

where k is determined from (8) below, whereas $\overline{E}_0$ and $\overline{H}_0$ are constant (i.e., $\overline{r}$ independent) vectors. In connection with this field, (2) yield the homogeneous algebraic system

$$\begin{aligned}(-k_\rho^2 + k_\epsilon^2)E_{0z} &= -j\omega\mu_0\mu_3\nu H_{0z}\\ (-k_\rho^2 + k_\mu^2)H_{0z} &= j\omega\epsilon_0\epsilon_3\nu E_{0z}; \quad k_\rho^2 = k_x^2 + k_y^2\end{aligned} \tag{7}$$

$(E_{0z} = \hat{z}\cdot\overline{E}_0, H_{0z} = \hat{z}\cdot\overline{H}_0)$. From (7), one gets the following bi-quadratic with respect to k dispersion equation:

$$Ak^4 + Bk^2 + C = 0 \tag{8}$$

where $A = \sin^4\vartheta_0 + (\epsilon_3/\epsilon_1 + \mu_3/\mu_1)\sin^2\vartheta_0\cos^2\vartheta_0 + \epsilon_3\mu_3/(\epsilon_1\mu_1)\cos^4\vartheta_0$, $B = -k_0^2\{(\epsilon_3\mu_e + \mu_3\epsilon_e)\sin^2\vartheta_0 + 2\epsilon_3\mu_3[1 + \epsilon_2\mu_2/(\epsilon_1\mu_1)]\cos^2\vartheta_0\}$, $C = k_0^4\epsilon_3\mu_3\epsilon_e\mu_e$.

For a given value of ϑ_0, (8) specifies two values for k^2 denoted by $(k^+)^2$ and $(k^-)^2$, implying the two modeness of wave propagation in a gyrotropic space. In the sequel, we shall refer to the $(\pm)$-incident mode, characterized by the wavenumber $k^\pm$. To assure that both modes are nonevanescent the conditions $(k^+)^2(k^-)^2 > 0$ and $(k^+)^2 + (k^-)^2 > 0$ must be imposed. In view of (8), these two conditions imply the constrains $AC > 0$ and $BA < 0$, which restrict the band of the allowable operating frequencies.

Knowledge of $k^\pm$ via (8) suffices to completely determine both $(\overline{k}^\pm)^{\text{inc}}$ and, via (4), the field of the incident $(\pm)$ mode.

C. Formulation of the Boundary-Value Problem

Let us work in the Fourier transform domain defined by $\tilde{F}(u, y) = (1/2\pi)\int_{-\infty}^{\infty} F(x, y)e^{jux}\,dx$, $F(x, y) = \int_{-\infty}^{\infty}\tilde{F}(u, y)e^{-jux}\,du$. Then, with respect to the scattered field $(\overline{E}^{\text{scat}}, \overline{H}^{\text{scat}}) = [\overline{E}(x, y), \overline{H}(x, y)]e^{-j\beta z}$ (2) recast as

$$\begin{aligned}\left(\frac{d^2}{dy^2} + k_e^2\right)\tilde{E}_z(u, y) &= -j\omega\mu_0\mu_3\nu\tilde{H}_z(u, y)\\ \left(\frac{d^2}{dy^2} + k_m^2\right)\tilde{H}_z(u, y) &= j\omega\epsilon_0\epsilon_3\nu\tilde{E}_z(u, y)\end{aligned} \tag{9}$$

$k_e^2 = k_\epsilon^2 - u^2$, $k_m^2 = k_\mu^2 - u^2$. From (9), we get the decoupled equations

$$\left(\frac{d^2}{dy^2} + k_e^2\right)\left(\frac{d^2}{dy^2} + k_m^2\right)\tilde{G}_z = k_0^2\epsilon_3\mu_3\nu^2\tilde{G}_z \quad (G \equiv E, H) \tag{10}$$

whose general solution at points of regions 1 $(y > 0)$ and 2 $(y < 0)$ can be written as

$$\tilde{H}_{zi}(u, y) = A_i\exp(\mp j\tau_a y) + B_i\exp(\mp j\tau_b y) = \tilde{H}_{zi}^a + \tilde{H}_{zi}^b \tag{11a}$$

$$\begin{aligned}\tilde{E}_{zi}(u, y) &= jZ_aA_i\exp(\pm j\tau_a y) + jZ_bB_i\exp(\mp j\tau_b y)\\ &= \tilde{E}_{zi}^a + \tilde{E}_{zi}^b\end{aligned} \tag{11b}$$

for $i = 1$ (upper sign), 2 (lower sign). Here A_i, B_i $(i = 1, 2)$ are expansion constants to be determined and

$$\begin{aligned}\tau_a^2 &= \tfrac{1}{2}(k_e^2 + k_m^2 + \delta) = k_a^2 - u^2\\ \tau_b^2 &= \tfrac{1}{2}(k_e^2 + k_m^2 - \delta) = k_b^2 - u^2\\ \delta &= [(k_\epsilon^2 - k_\mu^2)^2 + 4k_0^2\epsilon_3\mu_3\nu^2]^{1/2}\end{aligned} \tag{12}$$

$$k_a^2 = \tfrac{1}{2}(k_\epsilon^2 + k_\mu^2 + \delta), \quad k_b^2 = \tfrac{1}{2}(k_\epsilon^2 + k_\mu^2 - \delta). \tag{13}$$

For δ, any of its branches may be selected (being fixed thereafter). The proper branches of the double-valued functions $\tau_q(u)$ $(q \equiv a, b)$, on the other hand, have to be selected in accordance with the radiation condition $\text{Im}\{\tau_q(u)\} < 0$. (For a detailed examination of the analytical properties of $\tau_q(u)$ on the complex u plane refer to [4] and [5]). Finally, for the quantities $Z_q = -j\tilde{E}_z^q/\tilde{H}_z^q$ $(q \equiv a, b)$ introduced in (11b) one obtains

$$\begin{aligned}Z_a &= (k_\epsilon^2 - k_\mu^2 + \delta)/(2\omega\epsilon_0\epsilon_3\nu)\\ Z_b &= (k_\epsilon^2 - k_\mu^2 - \delta)/(2\omega\epsilon_0\epsilon_3\nu).\end{aligned} \tag{14}$$

As seen, Z_a and Z_b depend on the physical parameters solely, being independent of the spectral variable u.

In terms of $\tilde{E}_{zi}$ and $\tilde{H}_{zi}$ the expressions of $\tilde{E}_{xi}$ and $\tilde{H}_{xi}$ $(i = 1, 2)$ may be derived with the help of (4).

From the boundary conditions for E_z, H_z, E_x, H_x at $y = 0$ one gets

$$A_1Z_a + B_1Z_b = A_2Z_a + B_2Z_b, \quad A_1 + B_1 = A_2 + B_2 + \tilde{J}_x(u)$$

$$\begin{aligned}\tau_aP_a(A_1 + A_2) + \tau_bP_b(B_1 + B_2) &= -jup\tilde{J}_x(u)\\ \tau_aQ_a(A_1 + A_2) + \tau_bQ_b(B_1 + B_2) &= ju\sigma\tilde{J}_x(u) + j\Delta\tilde{J}_z(u)\end{aligned} \tag{15}$$

where

$$\Delta = \nu^2 + \upsilon\hat{\upsilon}, \quad p = \frac{\beta\nu}{\omega\epsilon_0\epsilon_1} - j\frac{\epsilon_2}{\epsilon_1}\upsilon, \quad \sigma = \nu\frac{\mu_2}{\mu_1} + \frac{\beta k_\epsilon^2}{\mu_1\epsilon_3 k_0^2}$$
$$P_q = \nu Z_q + j\upsilon, \quad Q_q = \nu + j\hat{\upsilon}Z_q \qquad (q = a, b). \tag{16}$$

D. Formulation of the SIE-SIDE of the Problem

With the help of (15), one can express A_i and B_i $(i = 1, 2)$ in terms of $\tilde{J}_x(u)$ and $\tilde{J}_z(u)$. The result of a very lengthy algebraic procedure is then

$$\begin{aligned} 2\Delta(Z_a - Z_b)\tilde{E}_z(u, 0) &= u(R_a P_b \tau_a^{-1} - R_b P_a \tau_b^{-1})\tilde{J}_x(u) \\ &\quad + (Z_a P_b \tau_a^{-1} - Z_b P_a \tau_b^{-1})\Delta \tilde{J}_z(u) \\ 2\Delta(Z_a - Z_b)\tilde{E}_x(u, 0) &= \frac{1}{\Delta}\{(\tau_a Z_b P_a - \tau_b Z_a P_b)\Delta \\ &\quad - u^2[P_a Z_b^{-1}\tau_b^{-1}R_b^2 - P_b Z_a^{-1}\tau_a^{-1}R_a^2]\}\tilde{J}_x(u) \\ &\quad + u(R_a P_b \tau_a^{-1} - R_b P_a \tau_b^{-1})\tilde{J}_z(u) \end{aligned} \tag{17}$$

where for $q = a, b$

$$R_q = \sigma Z_q - p. \tag{18}$$

To get (17) the first of the identities in Appendix A was repeatedly used.

In the space domain, (17), after dividing both sides by $Z_a Z_b \Delta$ and using the third identity of Appendix A, take the following compact form:

$$\alpha E_z^{\text{inc}}(x, 0) = \sum_{q=a,b} s_q P_q^{-1}\left[Z_q \Delta L_q(J_z) + jR_q \frac{d}{dx}L_q(J_x)\right] \tag{19a}$$

$$\alpha E_x^{\text{inc}}(x, 0) = \sum_{q=a,b} s_q P_q^{-1}\left\{jR_q \frac{d}{dx}L_q(J_z) + \frac{1}{Z_q\Delta} \cdot \left[(P_q^2 - R_q^2)\frac{d^2}{dx^2} + k_q^2 P_q^2\right]L_q(J_x)\right\} \tag{19b}$$

$|x| \leq w$, where

$$\alpha = 4(Z_a^{-1} - Z_b^{-1}), \quad s_a = 1, \quad s_b = -1 \tag{20}$$
$$L_q(J) \equiv \int_{-w}^{w} J(x')H_0(k_q|x - x'|)\,dx'. \tag{21}$$

To get (19), the boundary condition $\hat{t}\cdot\overline{E}(x, 0) = -\hat{t}\cdot\overline{E}^{\text{inc}}(x, 0)$, $|x| \leq w$ $(\hat{t} \equiv \hat{x}, \hat{z})$ was also used along with the relations $(1/\pi)\int_{-\infty}^{\infty} \tau_q^n e^{-ju(x-x')}\,du = H_0(k_q|x - x'|)$; $n = -1$, $(k_q^2 + d^2/dx^2)H_0(k_q|x - x'|)$; $n = 1$ $(q \equiv a, b)$. [The Hankel function $H_0(\cdot)$ is of the second kind; k_q is determined from (13)].

An Alternative Formulation Technique: An independent space-domain Green's function approach, which again yields system (19), thus providing a test of its correctness, is outlined in Appendix B.

E. Solution of (19)

To determine J_x and J_z from (19) we shall independently use two of the algorithms developed in [3] as follows.

Method A: We set $x = wt$, $x' = w\tau$ $(-1 \leq t, \tau \leq 1)$, and use the expansions

$$J_z[x(t)] = \frac{F^z(t)}{\sqrt{1-t^2}} = \frac{1}{\sqrt{1-t^2}}\sum_{N=0}^{\infty} a_N T_N(t)$$
$$J_x[x(t)] = \sqrt{1-t^2}F^x(t) = \sqrt{1-t^2}\sum_{N=0}^{\infty} b_N U_N(t) \tag{22}$$

where T_N and U_N are the Chebyshev polynomials of the first and of the second kind. Insert (22) into (19). Multiply (19a) by $T_M(\tau)/\sqrt{1-\tau^2}$, (19b) by $\sqrt{1-\tau^2}U_M(\tau)$ $(M = 0, 1, 2, \cdots)$, and integrate from $\tau = -1$ to $\tau = 1$. The final result is the linear algebraic system of

$$\sum_{N=0}^{\infty}(a_N K_{MN}^{zz} + b_N K_{MN}^{zx}) = \alpha\pi c_M$$
$$\sum_{N=0}^{\infty}(a_N K_{MN}^{xz} + b_N K_{MN}^{xx}) = \alpha\pi d_M \tag{23}$$

$(M = 0, 1, 2, \cdots)$ where

$$\begin{aligned} K_{MN}^{zz} &= w\Delta \sum_{q=a,b} s_q P_q^{-1} Z_q A_{MN}^{(1)}(k_q w) \\ K_{MN}^{xz} &= j\sum_{q=a,b} s_q P_q^{-1} R_q C_{MN}^{(1)}(k_q w) = -K_{NM}^{zx} \\ K_{NM}^{xx} &= \frac{1}{w\Delta}\sum_{q=a,b} s_q P_q^{-1} Z_q^{-1}(P_q^2 - R_q^2)D_{MN}^{(1)}(\kappa_q^2, k_q w) \end{aligned} \tag{24}$$

$$\kappa_q^2 = k_q^2 P_q^2/(P_q^2 - R_q^2) \tag{25a}$$
$$c_M = E_{0z} j^M J_M(k_x w)$$
$$d_M = E_{0x}(M + 1)j^M J_{M+1}(k_x w)/(k_x w) \tag{25b}$$

with $J_M(\cdot)$ denoting the Bessel function of order M. $A_{MN}^{(1)}$, $C_{MN}^{(1)}$, $D_{MN}^{(1)}$ are given in [3], whereas corresponding to the $\pm$ incident mode

$$E_{0x} = \frac{1}{\Delta}[(-j\nu + \upsilon/Z^{\pm})k_y + (-\sigma + p/Z^{\pm})k_x]E_{0z} \tag{26a}$$
$$Z^{\pm} \equiv -jE_{0z}/H_{0z} = \omega\mu_0\mu_3\nu/(k_\rho^2 - k_\epsilon^2)$$
$$= (k_\rho^2 - k_\mu^2)/(\omega\epsilon_0\epsilon_3\nu). \tag{26b}$$

Method B: This technique based on rather different principles [3], ends up with a linear algebraic system with the values $\{F^z(t_n), F^x(\hat{t}_n); n = 1, 2, \cdots, L\}$ [see (22)] as the unknowns. Here $t_n = \cos[(2n-1)\pi/(2L)]$ and $\hat{t}_n = \cos[n\pi/(L+1)]$ are zeros of $T_L(t)$ and $U_L(t)$, respectively, while the integer L is as high as needed to ensure convergence of (30) below. Leaving aside all intermediate derivations the final result is

$$\sum_{n=1}^{L}[R_{mn}^{zz}F^z(t_n) + R_{mn}^{zx}F^x(\hat{t}_n)] = j\pi\frac{\alpha}{2}\tilde{c}_m$$
$$\sum_{n=1}^{L}[R_{mn}^{xz}F^z(t_n) + R_{mn}^{xx}F^x(\hat{t}_n)] = j\pi\frac{\alpha}{2}\tilde{d}_m \tag{27}$$

$(m=1,2,\cdots,L)$, where

$$R_{mn}^{zz}=w\Delta\sum_{q=a,b}s_qP_q^{-1}Z_q\tilde{A}_{mn}^{(1)}(k_qw)$$

$$R_{mn}^{xx}=\frac{1}{w\Delta}\sum_{q=a,b}s_qP_q^{-1}Z_q^{-1}(P_q^2-R_q^2)\tilde{D}_{mn}^{(1)}(\kappa_q^2,k_qw)$$

$$R_{mn}^{zx}=j\sum_{q=a,b}s_qP_q^{-1}R_q\tilde{B}_{mn}^{(1)}(k_qw)$$

$$R_{mn}^{xz}=j\sum_{q=a,b}s_qP_q^{-1}R_q\tilde{C}_{mn}^{(1)}(k_qw) \quad (28)$$

$$\tilde{c}_m=E_{0z}\exp(jk_xwt_m),\quad \tilde{d}_m=E_{0x}\exp(jk_xw\hat{t}_m) \quad (29)$$

with $\tilde{F}_{mn}^{(1)}$ $(F=A,B,C,D)$ given in [3].

In terms of $F^z(t_n)$ and $F^x(\hat{t}_n)$, J_z and J_x are given by [3]

$$J_z[x(t)]=\frac{1}{\sqrt{1-t^2}}\,\frac{1}{L}\sum_{N=0}^{L-1}(2-\delta_{N0})T_N(t)\cdot\sum_{n=1}^{L}T_N(t_n)F^z(t_n) \quad (30a)$$

$$J_x[x(t)]=\frac{2}{L+1}\,\sqrt{1-t^2}\sum_{N=0}^{L-1}U_N(t)\cdot\sum_{n=1}^{L}(1-\hat{t}_n^2)U_N(\hat{t}_n)F^x(\hat{t}_n) \quad (30b)$$

$(\delta_{N0}=0,\ N\neq 0,\ \delta_{00}=1)$. Equation (22) and for sufficiently large values of L, (30) should yield coinciding results thus providing a validity test for both algorithms.

F. Far- and Near-Scattered Fields

The z components of the scattered field are the inverse Fourier transforms of (11). At points $\overline{r}(x,y,z)=\overline{\rho}(\rho,\phi)+\hat{z}z$ far from the strip $(\rho\to+\infty)$ the stationary phase asymptotic integration technique [6] yields

$$\begin{pmatrix}E_z^{\text{scat}}(\overline{\rho},z)\\ H_z^{\text{scat}}(\overline{\rho},z)\end{pmatrix}=e^{-j\beta z}\sum_{q=a,b}s_q\frac{e^{-jk_q\rho}}{\sqrt{\rho}}\begin{pmatrix}1\\ -j/Z_q\end{pmatrix}F_q(\phi)$$

$$F_q(\phi)=\frac{\sqrt{j2\pi}}{2(Z_a-Z_b)}Z_q\cdot\left\{-j\sqrt{k_q}Z^q\sin\phi\tilde{J}_x(u_q)+\frac{1}{\sqrt{k_q}}\cdot\left[\frac{u_q}{\Delta}(\sigma P^q+pQ^q)\tilde{J}_x(u_q)+P^q\tilde{J}_z(u_q)\right]\right\} \quad (31)$$

where $u_q=k_q\cos\phi$ $(0\leq\phi\leq 2\pi)$, $\{T^a=T_b,\ T^b=T_a\ (T\equiv Z,P,Q)\}$. $\tilde{J}_z(u)$ and $\tilde{J}_x(u)$, the Fourier transforms of $J_z(x)$ and $J_x(x)$, are given by

$$\tilde{J}_z(u)=\frac{w}{2}\sum_{N=0}^{\infty}a_Nj^NJ_N(wu)=\frac{w}{2L}\sum_{n=1}^{L}F^z(t_n)\exp(juwt_n)$$

$$\tilde{J}_x(u)=\frac{w}{4}\sum_{N=0}^{\infty}b_Nj^N[J_N(wu)+J_{N+2}(wu)]=\frac{w}{2(L+1)}\sum_{n=1}^{L}(1-\hat{t}_n^2)F^x(\hat{t}_n)\exp(juw\hat{t})_n) \quad (32)$$

in terms of either $\{a_n,b_n\}$ or $\{F^z(t_n),\ F^x(\hat{t}_n)\}$. The second part of each of (32) has been based on Lobatto's integration formulas [7].

The other components of this field can be found from (4) using (31).

Remarks:

1) As seen, the far-scattered field is composed of two waves (labeled as a and b) with "radiation patterns" $F_a(\phi)$ and $F_b(\phi)$, respectively.
2) Equations (31) can alternatively be deduced from (B.7) and (B.10) as follows: setting $R=[(x-x')^2+y^2]^{1/2}=\rho-x'\cos\phi\ (\rho\to\infty)$ and replacing $H_0(k_qR)$ in (B.8) by its large argument asymptotic expression yields

$$\mathcal{L}_q(J)=\sqrt{j\frac{2}{\pi k_q\rho}}e^{-jk_q\rho}\int_{-w}^{w}J(x')e^{jk_qx'\cos\phi}\,dx'=2\pi\sqrt{j\frac{2}{\pi k_q\rho}}e^{-jk_q\rho}\tilde{J}(k_q\cos\phi)$$

$J\equiv J_z,J_x$. Substituting into each of (B.7) and (B.10), setting $(\partial/\partial x)=\cos\phi(\partial/\partial\rho)-(\sin\phi/\rho)(\partial/\partial\phi),(\partial/\partial y)=\sin\phi(\partial/\partial\rho)+(\cos\phi/\rho)(\partial/\partial\phi)$, evaluating the indicated derivatives, and retaining only terms whose amplitude varies as $\rho^{-1/2}$, we again arrive at (31).

For the far-scattered power, carrying out the integration $P^{\text{scat}}=\frac{1}{2}\text{ Re }\int_{-w}^{w}\tilde{J}^*(x)\cdot\overline{E}^{\text{scat}}(x,0)dx=-\frac{1}{2}\text{Re}\int_{-w}^{w}\overline{J}^*(x)\cdot\overline{E}^{\text{inc}}(x,0)dx$ we get the relation $P^{\text{scat}}/w=-(\pi/2)\text{ Re }\Sigma_{N=0}^{\infty}(a_N^*c_N+b_N^*d_N)$ with c_N and d_N given by (25b). (* denotes the conjugate of a complex number).

Analytical expressions may be derived for the scattered field near the strip as well. Thus, in order to evaluate $E_z^{\text{scat}}(x,y)$ and $H_z^{\text{scat}}(x,y)$, one simply has to set

$$\mathcal{L}_q(J_z)=\frac{\pi}{L}w\sum_{n=1}^{L}\Gamma^z(t_n)H_0(k_qR)$$
$$R=\sqrt{(x-wt_n)^2+y^2} \quad (33)$$

$$\frac{\partial}{\partial p}\mathcal{L}_q(J_x)=\frac{\pi w}{L+1}k_q\sum_{n=1}^{L}\frac{\partial\hat{R}}{\partial p}(1-\hat{t}_n^2)\Gamma^x(\hat{t}_n)H_0'(k_q\hat{R})\quad (p\equiv x,y)$$
$$\hat{R}=\sqrt{(x-w\hat{t}_n)^2+y^2} \quad (34)$$

in each of (B.7) and (B.10). The quantities Γ^x and Γ^z are given either by $\{\Gamma^z(t_n)\equiv F^z(t_n),\ \Gamma^x(\hat{t}_n)\equiv F^x(\hat{t}_n)\}$, in the context of method B or by $\{\Gamma^z(t_n)=\Sigma_{N=0}^{\infty}a_N\cos(N\Theta_n),\ \Gamma^x(\hat{t}_n)=\Sigma_{N=0}^{\infty}b_N\sin[(N+1)\hat{\Theta}_n]/\sin(\hat{\Theta}_n);\ \Theta_n=(2n-1)\pi/(2L),\ \hat{\Theta}_n=n\pi/(L+1)\}$ in the context of method A.

[In the former case, L in (33) and (34) is specified from the beginning; in the latter case, L may assume any convenient value irrespective of the truncation size use for system (23)]. Results (33) and (34) were based on Lobatto's integration formulas; $H_0'(\cdot)$ in (34) denotes the derivative with respect to argument.

III. Scattering by a Strip in a Bi-Isotropic Space

Let the strip in Fig. 1 be now embedded in the unbounded lossless biisotropic space $(\epsilon, \mu, \zeta, \xi)$ described by the constitutive relations $\overline{D} = \epsilon_0(\epsilon\overline{E} + Z_0\xi\overline{H})$, $\overline{B} = \mu_0(Y_0\zeta\overline{E} + \mu\overline{H})$; $Z_0 = 1/Y_0 = \sqrt{\mu_0/\epsilon_0}$. According to the lossless condition, $\xi = \chi - j\kappa = \zeta^*$, where the dimensionless parameters χ (Pasteur) and κ (Tellegen) serve as measures of the degree of chirality and nonreciprocity of the medium, respectively. Just like ϵ and μ, χ is an even function of frequency, whereas κ is an odd one. The practical case $\xi = \zeta = \chi$ $(\kappa = 0)$ of a chiral medium results in as a special case.

Assume a plane wave obliquely incident on the strip. The induced current density $\overline{J} = \hat{x}J_x + \hat{z}J_z$ gives rise to the scattered field. All these field quantities vary as $e^{-j\beta z}$ where β is specified by the incident wave as outlined in Section III-B below.

This quasi two-dimensional problem may be formulated in terms of a system of coupled SIE-SIDE along the lines outlined in the preceding section. This possibility is based on (and also reflects) the strong similarities that exist between these two problems.

A. Basic Equations

Solutions to the source-free Maxwell's equations $\nabla \times \overline{E} = -j\omega\overline{B}$, $\nabla\times\overline{H} = j\omega\overline{D}$ that vary as $e^{j(\omega t-\beta z)}$ can be expressed in terms of their longitudinal components E_z and H_z satisfying the equations analogous to (2)

$$\begin{aligned}(\nabla_t^2 + k_\zeta^2)E_z &= -\mu Z_0\nu H_z\\ (\nabla_t^2 + k_\xi^2)H_z &= \epsilon Y_0\nu E_z \end{aligned} \tag{35}$$

$$\begin{aligned}k_\zeta^2 &= k_0^2\epsilon\mu - \beta^2 - k_0^2\zeta^2\\ k_\xi^2 &= k_0^2\epsilon\mu - \beta^2 - k_0^2\xi^2\\ \nu &= k_0^2(\xi - \zeta).\end{aligned} \tag{36}$$

In terms of E_z and H_z the transverse components are given by

$$\begin{pmatrix}\overline{E}_t\\ \overline{H}_t\end{pmatrix} = j\begin{pmatrix}-k_\zeta^2 & -\nu\mu Z_0\\ \nu\epsilon Y_0 & -k_\xi^2\end{pmatrix}^{-1} \cdot\begin{pmatrix}-k_0\zeta\hat{z}\times\nabla_t + \beta\nabla_t & -\omega\mu_0\mu\hat{z}\times\nabla_t\\ \omega\epsilon_0\epsilon\hat{z}\times\nabla_t & k_0\xi\hat{z}\times\nabla_t + \beta\nabla_t\end{pmatrix} \cdot\begin{pmatrix}E_z\\ H_z\end{pmatrix}. \tag{37}$$

B. Incident Field

Let $(\overline{E}^{\text{inc}}, \overline{H}^{\text{inc}}) = (\overline{E}_0, \overline{H}_0)\exp(j\overline{k}^{\text{inc}}\cdot\overline{r})$ be the incident plane wave, propagating in the direction of $\overline{k}^{\text{inc}}(k, \partial_0, \phi_0)$ [see (6)] with k determined via (39) below. With respect to this field the equations analogous to (7) and (8) read as

$$(-k_\rho^2 + k_\zeta^2)E_{0z} = -\mu Z_0\nu H_{0z}, \quad (-k_\rho^2 + k_\xi^2)H_{0z} = \epsilon Y_0\nu E_{0z} \tag{38}$$

$$k^4 + (\xi^2 + \zeta^2 - 2\epsilon\mu)k^2k_0^2 + (\epsilon\mu - \zeta\xi)^2k_0^4 = 0. \tag{39}$$

Equation (39) specifies two values for k^2, denoted by $(k^+)^2$ and $(k^-)^2$, thus implying the two modeness of wave propagation in a bi-isotropic space. In the sequel, we shall refer to the $(\pm)$ incident mode characterized by the wavenumber $k^\pm$. To assure that both modes are nonevanescent the conditions $(k^+)^2(k^-)^2 > 0$ and $(k^+)^2 + (k^-)^2 > 0$ must be imposed. In view of (39), these two conditions imply the constrain $\xi^2 + \zeta^2 < 2\epsilon\mu \Rightarrow \chi^2 + \kappa^2 < \epsilon\mu$, which restricts the band of the allowable operating frequencies.

Knowledge of $k^\pm$ via (39) suffices to determine both $(\overline{k}^\pm)^{\text{inc}}$ and the field of the incident $(\pm)$ mode.

C. Formulation of the Boundary-Value Problem

In the Fourier transform domain the following equations analogous to (9) and (10) may be written for the scattered field $(\overline{E}^{\text{scat}}, \overline{H}^{\text{scat}}) = [\overline{E}(x,y), \overline{H}(x,y)]e^{-j\beta z}$

$$\begin{aligned}\left(\frac{d^2}{dy^2} + K_\zeta^2\right)\tilde{E}_z(u,y) &= -\mu Z_0\nu\tilde{H}_z(u,y)\\ \left(\frac{d^2}{dy^2} + K_\xi^2\right)\tilde{H}_z(u,y) &= \epsilon Y_0\nu\tilde{E}_z(u,y)\end{aligned} \tag{40}$$

$$\left(\frac{d^2}{dy^2} + K_\zeta^2\right)\left(\frac{d^2}{dy^2} + K_\xi^2\right)\tilde{G}_z = -\epsilon\mu\nu^2\tilde{G}_z \quad (G \equiv E, H) \tag{41}$$

where $K_\zeta^2 = k_\zeta^2 - u^2$, $K_\xi^2 = k_\xi^2 - u^2$. The general solution of (41) at points of regions 1 $(y > 0)$ and 2 $(y < 0)$ take the form of (11a) and, in place of (11b), $\tilde{E}_{zi}(u,y) = Z_aA_i\exp(\mp j\tau_a y) + Z_bB_i\exp(\mp j\tau_b y)$ where now

$$Z_i = \tilde{E}_z^i/\tilde{H}_z^i = -\frac{Z_0}{2\epsilon}\left[\xi + \zeta \pm \sqrt{(\xi+\zeta)^2 - 4\epsilon\mu}\right] \quad (i = a; \text{upper sign}, b; \text{lower sign}) \tag{42}$$

$$\begin{aligned}\tau_a^2 &= \frac{1}{2}\left(K_\zeta^2 + K_\xi^2 + \delta\right) = k_a^2 - u^2,\\ \tau_b^2 &= \frac{1}{2}\left(K_\zeta^2 + K_\xi^2 - \delta\right) = k_b^2 - u^2\end{aligned} \tag{43}$$

with $\delta = [(k_\zeta^2 - k_\xi^2)^2 - 4\epsilon\mu\nu^2]^{1/2} = \nu\sqrt{(\xi+\zeta)^2 - 4\epsilon\mu}$

$$k_a^2 = \tfrac{1}{2}(k_\zeta^2 + k_\xi^2 + \delta), \quad k_b^2 = \tfrac{1}{2}(k_\zeta^2 + k_\xi^2 - \delta). \tag{44}$$

For δ either of its branches may be used in (43) and (44) (fixed thereafter). The proper branches of the double-valued functions $\tau_i(u)$ $(i \equiv a, b)$ are selected according to the condition $\text{Im}\{\tau_i(u)\} < 0$.

D. Formulation of the SIE-SIDE of the Problem

Applying the boundary conditions at $y = 0$ and working as in Section II-D the following system analogous to (19) results in:

$$\alpha E_z^{\text{inc}}(x,0) = \sum_{i=a,b} s_i \left\{ \sigma_i \Delta L_i(J_z) + jZ_i\Psi_i \frac{d}{dx} L_i(J_x) \right\} \tag{45a}$$

$$\alpha E_x^{\text{inc}}(x,0) = \sum_{i=a,b} s_i \left\{ -jV_i \frac{d}{dx} L_i(J_z) + \Gamma_i \left(\kappa_i^2 + \frac{d^2}{dx^2} \right) L_i(J_x) \right\} \tag{45b}$$

where s_i $(i = a, b)$ has been defined in (20). Here the notation

$$\begin{aligned} \alpha &= -4\Delta D k_0 (Z_a - Z_b), \quad \Delta = k_\zeta^2 k_\xi^2 + \epsilon\mu\nu^2 \\ D &= \epsilon\mu - \zeta\xi, \quad \kappa_i^2 = -k_0^2 k_i^2 \sigma^i D/\Gamma_i \\ \Gamma_i &= U_i \Delta^{-1} - k_0^2 \sigma^i D, \quad U_i = R_i \Psi_i \\ \Psi_i &= Q^i \lambda - k_\zeta^2 \beta P^i, \quad P_i = qZ_i + \mu p Z_0 \\ Q_i &= \hat{q} - Y_0 p \epsilon Z_i, \quad R_i = k_\xi^2 \beta Z_i + \lambda, \quad \sigma_i = Z_i P^i \\ V_i &= R_i P^i, \quad q = -k_\xi^2 \zeta - \epsilon\mu\nu, \quad p = -k_\xi^2 - \xi\nu \\ \hat{q} &= k_\zeta^2 \xi - \epsilon\mu\nu, \quad \lambda = -\nu\mu\beta Z_0 \end{aligned} \tag{46}$$

has been used, $\mathcal{F}^i$ $(\mathcal{F} \equiv Z, \sigma, Q, P)$ being shorthand symbols for $\mathcal{F}_b$ $(i = a)$ or $\mathcal{F}_a$ $(i = b)$.

An Alternative Formulation Technique: An independent approach, based on space-domain Green's functions combined with the modified reciprocity theorem is applicable, yielding again the system of SIE-SIDE (45). The medium complementary to $(\epsilon, \mu, \zeta, \xi)$ is now described by the scalars $(\epsilon, \mu, -\xi, -\zeta)$ [9]. The equations analogous to (B.7) and (B.10) in this case read as

$$-\alpha E_z(\overline{\rho}) = \sum_{i=a,b} s_i \left[-Z^i \hat{P}^i \Delta \mathcal{L}_i(J_z) - j\hat{P}^i \left(\hat{R}_i \frac{\partial}{\partial x} + k_0 \hat{P}_i \frac{\partial}{\partial y} \right) \mathcal{L}_i(J_x) \right] \tag{47}$$

$$-\alpha H_z(\overline{\rho}) = \sum_{i=a,b} s_i \hat{Q}^i \left[Z^i \Delta \mathcal{L}_i(J_z) + j \left(\hat{R}_i \frac{\partial}{\partial x} + k_0 \hat{P}_i \frac{\partial}{\partial y} \right) \mathcal{L}_i(J_x) \right] \tag{48}$$

with $\hat{P}_i$, $\hat{R}_i$, $\hat{Q}_i$ defined in Appendix C and $\{\hat{\mathcal{F}}^i = \hat{\mathcal{F}}_b$ $(i = a)$, $\hat{\mathcal{F}}_a$ $(i = b)$; $\mathcal{F} \equiv P, Q\}$.

From (47) and (48), one can reproduce both of (45) following step by step the procedure outlined in Appendix B with respect to the preceding gyrotropic problem. This task is facilitated by the set of identities listed in Appendix C.

E. Solution of (45)

From (45) via (22) working in the context of methods A and B, one arrives again at systems (23) and (27) where now a is given by the first of (46) whereas

$$\begin{aligned} K_{MN}^{zz} &= w\Delta \sum_{i=a,b} s_i \sigma_i A_{MN}^{(1)}(k_i w) \\ K_{MN}^{xz} &= j \sum_{i=a,b} s_i Z_i \Psi_i C_{MN}^{(1)}(k_i w) = -K_{NM}^{zx} \\ K_{MN}^{xx} &= \frac{1}{w} \times \sum_{i=a,b} s_i \Gamma_i D_{MN}^{(1)}(\kappa_i^2, k_i w) \end{aligned} \tag{49}$$

$$\begin{aligned} R_{mn}^{zz} &= w\Delta \sum_{i=a,b} s_i \sigma_i \tilde{A}_{mn}^{(1)}(k_i w) \\ R_{mn}^{xx} &= \frac{1}{w} \sum_{i=a,b} s_i \Gamma_i \tilde{D}_{mn}^{(1)}(\kappa_i^2, k_i w) \\ R_{mn}^{xz} &= j \sum_{i=a,b} s_i Z_i \Psi_i \tilde{C}_{mn}^{(1)}(k_i w) \\ R_{mn}^{zx} &= j \sum_{i=a,b} s_i Z_i \Psi_i \tilde{B}_{mn}^{(1)}(k_i w) \end{aligned} \tag{50}$$

with κ_i^2 defined in (46). On evaluating the right sides in (23) and (27), we now use

$$\begin{aligned} E_{0x} &= -\frac{1}{\Delta} \left[\beta(-k_\xi^2 + \mu\nu Z_0/Z^\pm) k_x + k_0(q + \mu Z_0 p/Z^\pm) k_y \right] E_{0z} \\ Z^\pm &\equiv E_{0z}/H_{0z} = \frac{-\nu\mu Z_0}{-k_\rho^2 + k_\zeta^2} = \frac{-k_\rho^2 + k_\xi^2}{\nu\epsilon Y_0} \\ &= -\frac{Z_0}{2\epsilon} \left[\xi + \zeta \pm \sqrt{(\xi+\zeta)^2 - 4\epsilon\mu} \right]. \end{aligned} \tag{51}$$

F. Far- and Near-Scattered Fields

The z components of the far-scattered field are given by

$$\begin{aligned} \begin{pmatrix} E_z^{\text{scat}}(\overline{\rho}, z) \\ H_z^{\text{scat}}(\overline{\rho}, z) \end{pmatrix} &= e^{-j\beta z} \sum_{i=a,b} s_i \frac{e^{-jk_i\rho}}{\sqrt{\rho}} \begin{pmatrix} 1 \\ 1/Z_i \end{pmatrix} F_i(\phi) \\ F_i(\phi) &= -\frac{2}{\alpha} \sqrt{j2\pi} \left\{ -\frac{1}{\sqrt{k_i}} Z^i \Delta \hat{P}^i \tilde{J}_z(u_i) - \sqrt{k_i} \hat{P}^i (\hat{R}_i \cos\phi + k_0 \hat{P}_i \sin\phi) \tilde{J}_x(u_i) \right\} \end{aligned} \tag{52}$$

$u_i = k_i \cos\phi$ $(0 \le \phi \le 2\pi)$, with $\tilde{J}_z(u)$ and $\tilde{J}_x(u)$ given by (32). The other components of this field can be found from (37). As seen the far-scattered field is composed of two waves with "radiation patterns" $F_a(\phi)$ and $F_b(\phi)$, respectively, in complete analogy with the preceding gyrotropic case.

Analytical expressions for the scattered field near the strip may also be found after substituting $\mathcal{L}_q(J_z)$ and $(\partial/\partial\ell)\mathcal{L}_q(J_x)$ $(\ell \equiv x, y)$ in (47) and (48) from (33) and (34).

IV. Numerical Examples

Figs. 2–4 refer to a strip embedded in a lossless ferrite medium that becomes anisotropic by means of a superimposed dc (bias) field $\overline{H}_{\text{dc}} = \hat{z} H_{\text{dc}}$. This medium is described by a scalar dielectric permittivity $\epsilon = \epsilon_0 \epsilon_r$ in addition to a tensorial magnetic permeability given by the second of (1) where $\mu_1 = 1 + \omega_0\omega_m/(\omega_0^2 - \omega^2)$, $\mu_2 = -\omega\omega_m/(\omega_0^2 - \omega^2)$,

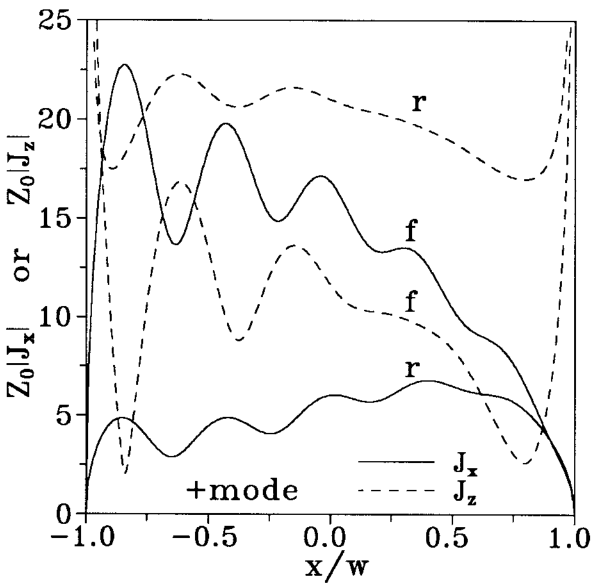

Fig. 2. $Z_0|J_x|$ and $Z_0|J_z|$ versus x/w for a strip in an anisotropic ferrite ($2w = \lambda_0$, $fr = 30$ GHz, $\phi_0 = \vartheta_0 = 45°$, $\epsilon_r = 16$, $\omega_0/\omega_m = 0.1124$) illuminated by the $+$ incident mode when $\overline{H}_{\rm dc} = \hat{z}H_{\rm dc}$ (curves labeled "f") or $\overline{H}_{\rm dc} = -\hat{z}H_{\rm dc}$ (curves labeled "r").

$\mu_3 = 1$. Here, $\omega_0 = \gamma H_{\rm dc}$, $\omega_m = \gamma M_s$, $\gamma \simeq 1.76 \times 10^{11}$ C/Kg being the magnetomechanical ratio and M_s the intensity of the saturation magnetization. We note that reversal in the direction of $\overline{H}_{\rm dc}$ results in a change of the sign of μ_2. In all these examples, the operating frequency was taken to be 30 GHz, while $\mu_0 M_s = 0.3$ Wb/m^2, $\epsilon_r = 16$, $\vartheta_0 = \phi_0 = 45°$, $2w = \lambda_0$ ($\lambda_0 =$ free-space wavelength), $\omega_0/\omega_m = 0.1124$.

Fig. 2 shows $Z_0|J_z|$ and $Z_0|J_x|$ as a function of x/w in the case of $(+)$ incident mode primary excitation. The curves labeled as "f" and "r," corresponding to the cases $\overline{H}_{\rm dc} = \hat{z}H_{\rm dc}$ and $\overline{H}_{\rm dc} = -\hat{z}H_{\rm dc}$, bring to light the effect of nonreciprocity.

Fig. 3, on the other hand, shows the radiation patterns of the far-scattered field. The waves labeled as (p^+) and (p^-) ($p = +$ or $p = -$), excited by the incident (p) mode, correspond to $F_a(\phi)$ and $F_b(\phi)$, respectively, given by (31). Finally, for the same parameter values, Fig. 4 shows $|E_z^{\rm tot}(x,y,z)|$ along the y axis ($x = 0, z = 0$) both for $(+)$mode (dashed curve) and $(-)$ mode (solid curve) primary excitations.

We note that as a partial test of the correctness of the numerical codes, all results presented in Figs. 2–4 were reproduced by methods A and B independently.

The convergence characteristics of the algorithms are illustrated in Table I where for the $+$ incident mode, $Z_0|J_x(x)|$, and $Z_0|J_z(x)|$ are shown along with elapsed CPU time for several values of $N_{\max}$ (the number of basis functions used in each of (22); method A) or L (see (27); method B). Here, $x = w/2$, $\epsilon_r = 9$, and $2w = \lambda_0/2$, the other parameter values being the same as in Figs. 2–4. The most important feature of Algorithm A is its exponential very stable convergence. For $N_{\max} = (10, 15, 20)$, for instance, the computed values are correct to within (5, 10, 16) significant decimals for both current densities. Method B, on the other hand, yields numerical values which, for increasing values of L, monotonically and asymptotically approach those of method A. (For a detailed comparison between these two methods refer to [3]).

The results presented in Figs. 5 and 6 refer to a strip in a chiral medium characterized by $\epsilon = 4$, $\mu = 1.5$, $\xi = \zeta = 0.3$ for $2w = \lambda_0$, $\phi_0 = \vartheta_0 = 45°$. Fig. 5 shows the radiation patterns of the far scattered waves. These waves labeled as (p^+) and (p^-) ($p \equiv_+$ or $p \equiv_-$) and excited by the incident (p)-mode, respectively, correspond to $F_a(\phi)$ and $F_b(\phi)$ given by (52). Finally, Fig. 6 shows $|E_z^{\rm tot}(x,y,z)|$ along the y axis. In this case, the $(+)$ and $(-)$ incident mode excitations yield coinciding results.

V. Conclusion

SIE techniques have been applied to study scattering by a conducting strip embedded in unbounded gyrotropic or bi-isotropic spaces. The governing SIE-SIDE were derived and discretized by two independent to one another methods. The present analysis may be used as a basis for treating more complicated strip-loaded bi-isotropic/anisotropic structures.

Appendix A
Useful Identifies for the Gyrotropic Case

For $q = a, b$; $m = a, b$; and $m \neq q$ we have

$$\begin{aligned} Z_m Q_q &= -P_q, \quad Z_q(-\nu P_m + jQ_m \upsilon) = -\Delta Z_a Z_b \\ \Delta Z_a Z_b &= P_a P_b, \quad Z_q(\sigma P_m + pQ_m) = P_m R_q \\ Q_m P_q &= -\Delta Z_m, \quad \nu P_a P_b + j\upsilon Q_m P_q = \Delta Z_m P_q \end{aligned}$$

$$\begin{aligned} \sigma P_m R_q + pQ_m R_q &= R_q^2 P_m / Z_q \\ j(-\nu P_m R_q + \sigma P_a P_b) - Q_m(\upsilon R_q + jpP_q) &= 0 \\ -R_q^2 P_m/Z_q + \Delta Z_m P_q &= \Delta Z_m (P_q^2 - R_q^2)/P_q. \end{aligned}$$

All symbols involved here refer to quantities defined in Section II.

Appendix B
Green's Function-Based Alternative Formulation Technique

Let $[\overline{\mathcal{E}}^J(\overline{\rho},\overline{\rho}')$, $\overline{\mathcal{H}}^J(\overline{\rho},\overline{\rho}')]e^{j\beta z}$, and $[\overline{\mathcal{E}}^M(\overline{\rho},\overline{\rho}')$, $\overline{\mathcal{H}}^M(\overline{\rho},\overline{\rho}')]e^{j\beta z}$ be the response at $\overline{\rho}(x,y)$ due to the unit phased-line sources $\overline{J}_u = I\delta(\overline{\rho}-\overline{\rho}')e^{j\beta z}$ ($I = 1$ A) and $\overline{M}_u = M\delta(\overline{\rho}-\overline{\rho}')e^{j\beta z}$ ($M = 1$ V), respectively, impressed at $\overline{\rho}'(x',y')$ inside the transposed (complementary) medium $(\overline{\overline{\epsilon}}^T, \overline{\overline{\mu}}^T)$. Then [8]

$$\begin{aligned} \mathcal{E}_z^G(\overline{\rho},\overline{\rho}') &= \sum_{q=a,b} \mathcal{E}_{zq}^G(\overline{\rho},\overline{\rho}') \\ \mathcal{H}_z^G(\overline{\rho},\overline{\rho}') &= \sum_{q=a,b} \mathcal{H}_{zq}^G(\overline{\rho},\overline{\rho}'); \qquad G \equiv J, M \end{aligned} \tag{B.1}$$

$$\mathcal{E}_{zq}^G(\overline{\rho},\overline{\rho}') = jZ_q \mathcal{H}_{zq}^G(\overline{\rho},\overline{\rho}') \tag{B.2}$$

$$\begin{aligned} \mathcal{H}_{zq}^G(\overline{\rho},\overline{\rho}') = &-\frac{s_q}{4(Z_a - Z_b)}\,(jP^q I\delta_{GJ} + Q^q M\delta_{GM}) \\ &\cdot H_0(k_q|\overline{\rho}-\overline{\rho}'|) \end{aligned} \tag{B.3}$$

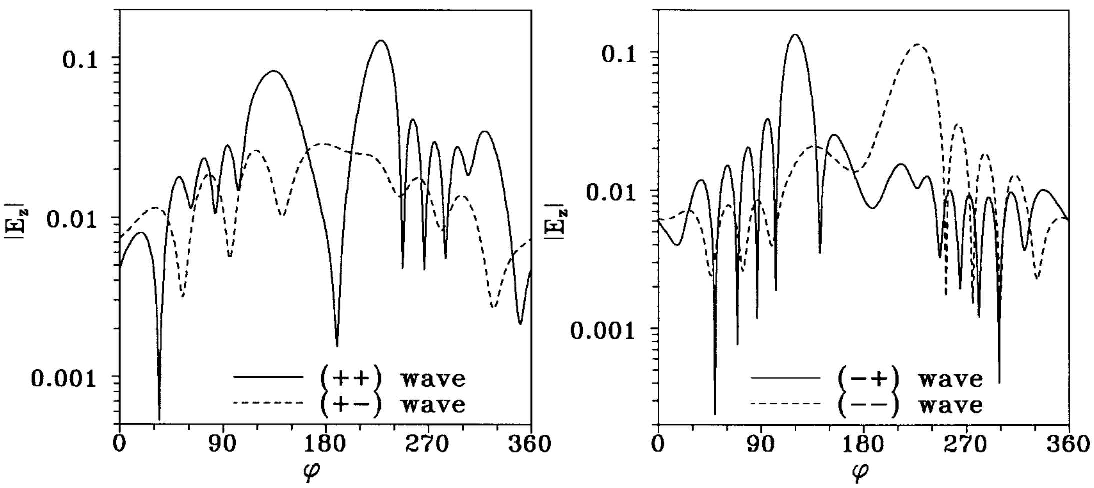

Fig. 3. Radiation patterns of the $(++)$, $(+-)$, $(-+)$, and $(--)$ waves when the strip is embedded in an anisotropic ferrite for the same parameter values as in Fig. 2.

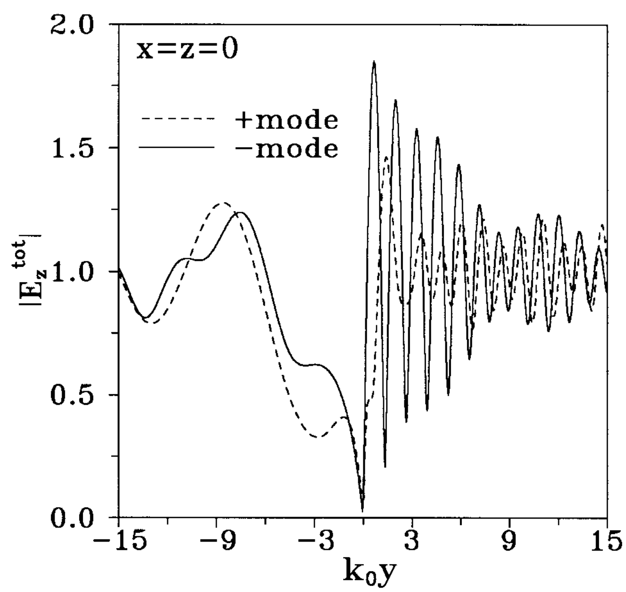

Fig. 4. Near-field $|E_z^{\rm tot}(0, y, 0)|$ versus $k_0 y$ for the same parameter values as in Fig. 2.

TABLE I
CONVERGENCE OF THE ALGORITHMS

Method A			
N_{max}	$Z_0\|J_x\|$	$Z_0\|J_z\|$	CPU
5	6.54	7.36	5
10	6.49026	7.552376	16
15	6.4902413289	7.552387316	36
20	6.490241328440637	7.552387318106955	88
∞	6.490241328440637	7.552387318106955	

Method B			
L	$Z_0\|J_x\|$	$Z_0\|J_z\|$	CPU
10	6.57269	7.78092	2
20	6.50827	7.60726	6
40	6.49431	7.56599	25
60	6.49199	7.55843	56
100	6.49085	7.55456	155
200	6.49039	7.55293	627

with $\{\mathcal{F}^a = \mathcal{F}_b,\ \mathcal{F}^b = \mathcal{F}_a\ (\mathcal{F} \equiv P, Q)\}$ and $\{\delta_{GQ} = 1\ (G \equiv Q),\ 0\ (G \not\equiv Q)\}$ $(s_q, Z_q, P_q, Q_q\ (q = a, b)$ have been defined in Sections II-B and C).

The modified reciprocity theorem [9] $\langle \overline{J}, \overline{J}_u \rangle = \langle \overline{J}_u, \overline{J} \rangle^c$, $\langle \overline{J}, \overline{M}_u \rangle = \langle \overline{M}_u, \overline{J} \rangle^c$ yields for the z components of the scattered field $(\overline{E}^{\rm scat}, \overline{H}^{\rm scat}) = [\overline{E}(x, y), \overline{H}(x, y)]e^{-j\beta z}$ the relations

$$E_z(\overline{\rho}) = \int_{-w}^{w} J_z(x')\mathcal{E}_z^J(x', 0; \overline{\rho})\, dx' + \int_{-w}^{w} J_x(x')\mathcal{E}_x^J(x', 0; \overline{\rho})\, dx' \tag{B.4}$$

$$-H_z(\overline{\rho}) = \int_{-w}^{w} J_z(x')\mathcal{E}_z^M(x', 0; \overline{\rho})\, dx' + \int_{-w}^{w} J_x(x')\mathcal{E}_x^M(x', 0; \overline{\rho})\, dx' \tag{B.5}$$

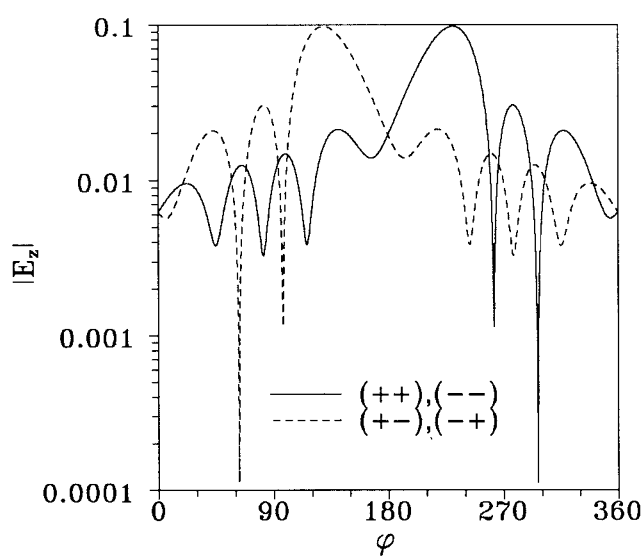

Fig. 5. Radiation patterns of the $(++)$, $(+-)$, $(-+)$, and $(--)$ waves when the strip is embedded in a chiral medium ($2w = \lambda_0$, $fr = 30$ GHz, $\phi_0 = \vartheta_0 = 45°$, $\epsilon = 4$, $\mu = 1.5$, $\xi = \zeta = 0.3$).

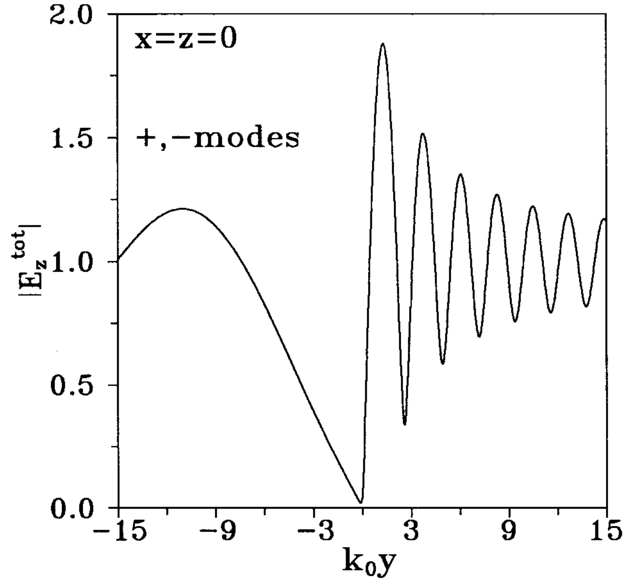

Fig. 6. Near field $|E_z^{\rm tot}(0, y, 0)|$ versus $k_0 y$ for the same parameter values as in Fig. 5.

where using (4) and taking into account the $\exp(j\beta z)$ dependence

$$\mathcal{E}_x^G(\overline{\rho}, \overline{\rho}') = \frac{1}{\Delta}\left(-\nu\frac{\partial}{\partial y} - j\sigma\frac{\partial}{\partial x}\right)\mathcal{E}_z^G + \frac{1}{\Delta}\left(\upsilon\frac{\partial}{\partial y} - p\frac{\partial}{\partial x}\right)\mathcal{H}_z^G \quad (G \equiv J, M). \quad \text{(B.6)}$$

Using (B.1)–(B.3) and (B.6), (B.4) yields

$$E_z(\overline{\rho}) = \frac{Z_a Z_b}{4(Z_a - Z_b)} \sum_{q=a,b} s_q\left[Z_q P_q^{-1}\Delta\mathcal{L}_q(J_z) + \left(jP_q^{-1}R_q\frac{\partial}{\partial x} + \frac{\partial}{\partial y}\right)\mathcal{L}_q(J_x)\right] \quad \text{(B.7)}$$

$$\mathcal{L}_q(J) = \int_{-w}^{w} J(x')H_0[k_q\sqrt{(x-x')^2 + y^2}]\,dx'. \quad \text{(B.8)}$$

Letting $y \to 0^{\pm}$ in (B.7) and using the relation

$$\lim_{y\to 0\pm}\left[\frac{\partial}{\partial y}\mathcal{L}_q(J)\right] = \pm 2jJ(x) \quad \text{(B.9)}$$

we again arrive at (19a) with the help of Appendix A equations.

From (B.5) we obtain the following equation analogous to (B.7):

$$H_z(\overline{\rho}) = \frac{1}{4\Delta(Z_a - Z_b)} \sum_{q=a,b} s_q Q^q\left[jZ_q\Delta\mathcal{L}_q(J_z) - \left(R_q\frac{\partial}{\partial x} + jP_q\frac{\partial}{\partial y}\right)\mathcal{L}_q(J_x)\right]. \quad \text{(B.10)}$$

Note: Letting $y \to 0^+$, $y \to 0^-$ successively in (B.10), subtracting the resulting equations, and applying the boundary condition $H_z(x, 0^+) - H_z(x, 0^-) = J_x(x)$, $|x| \le w$, results in the identity $J_x(x) = J_x(x)$; that is, (B.10) cannot be used directly to derive a second linearly independent integral equation.

Using (4) to express $E_x(\overline{\rho})$ in terms of $E_z(\overline{\rho})$ and $H_z(\overline{\rho})$ yields via (B.7), (B.10) the relation

$$4(Z_b^{-1} - Z_a^{-1})E_x(\overline{\rho}) = \sum_{q=a,b} s_q\left\{\left(jP_q^{-1}R_q\frac{\partial}{\partial x} - \frac{\partial}{\partial y}\right)\mathcal{L}_q(J_z) + \frac{1}{Z_q\Delta}P_q^{-1}\left[(P_q^2 - R_q^2)\frac{\partial^2}{\partial x^2} + k_q^2 P_q^2\right]\mathcal{L}_q(J_x)\right\}. \quad \text{(B.11)}$$

The algebraic manipulations in deriving (B.11) were simplified by using the set of identities given in Appendix A. Finally, setting $y = 0$ in (B.11) leads via (B.9) to (19b).

Appendix C
Useful Identifies for the Bi-Isotropic Case

$$Z_b(q\hat{P}_b - Z_0\mu p\hat{Q}_b) = Z_a(q\hat{P}_a - Z_0\mu p\hat{Q}_a) = -\Delta D Z_a Z_b,$$
$$Z_a Z_b = \frac{\mu}{\epsilon}Z_0^2 \quad \text{(C.1)}$$

$$Z_i\hat{P}_i = -\frac{\mu}{\epsilon}Z_0^2 Q_i, \quad Z_i\hat{Q}_i = P_i,$$
$$Z_i P^i = \frac{\mu}{\epsilon}Z_0^2\hat{Q}^i, \quad Z_i Q^i = -\hat{P}^i$$
$$Z_i P^i = -Z^i\hat{P}^i, \quad Z^i\hat{\Psi}_i = R_i P^i = V_i,$$
$$Z_i\Psi_i = -\hat{R}_i\hat{P}^i, \quad \hat{R}_i\hat{\Psi}_i = R_i\Psi_i$$
$$(i = a, b) \quad \text{(C.2)}$$

where $\hat{P}_i$, $\hat{Q}_i$, $\hat{\Psi}_i$, $\hat{R}_i$, the duals of P_i, Q_i, R_i, Ψ_i, are given by

$$\hat{P}_i = -Z^i\hat{q} + \mu p Z_0, \quad \hat{Q}_i = q + Y_0 p\epsilon Z^i$$
$$\hat{\Psi}_i = \hat{Q}^i\lambda - k_\xi^2\beta\hat{P}^i, \quad \hat{R}_i = -k_\zeta^2\beta Z^i + \lambda. \quad \text{(C.3)}$$

All symbols involved here refer to quantities defined in Section III.

References

[1] *J. Electromagn. Waves Applicat.—Special Issue Wave Interactions Chiral Complex Media*, vol. 6, no. 5/6, 1992.

[2] A. Sihvola, Ed., in *Proc. Bi-Isotropics Workshop Novel Microwave Materials*, Helsinki Univ. Technol., Finland, Feb. 1993.

[3] J. L. Tsalamengas, "Direct singular integral equation methods in scattering and propagation in strip or slot loaded structures," *IEEE Trans. Antennas Propagat.*, to be published.

[4] S. Przezdziecki and R. A. Hurd, "Diffraction by a half plane perpendicular to the distinguished axis of a gyrotropic medium (oblique incidence)," *Can. J. Phys.*, vol. 59, pp. 403–424, 1981.

[5] R. A. Hurd and S. Przezdziecki, "Half-plane diffraction in a gyrotropic medium," *IEEE Trans. Antennas Propagat.*, vol. AP-33, pp. 813–822, Aug. 1985.

[6] R. E Collin and F. J. Zucker, *Antenna Theory*. New York: McGraw-Hill, 1969.

[7] M. Abramowitz and I. A. Stegun, *Handbook of Mathematical Functions*. New York: Dover, 1972.

[8] N. Okamoto, "Scattering of obliquely incident plane waves from a finite periodic structure of ferrite cylinders," *IEEE Trans. Antennas Propagat.*, vol. AP-27, pp. 317–323, May 1979.

[9] J. A. Kong, *Electromagnetic Wave Theory*. New York: Wiley, 1986.

[10] J. C. Monzon, "Radiation and scattering in homogeneous general biisotropic regions," *IEEE Trans. Antennas Propagat.*, vol. 38, pp. 227–235, Feb. 1990.

J. L. Tsalamengas (S'76–M'87), photograph and biography not available at the time of publication.